

Received: 26 February 2013 – Accepted: 28 February 2013 – Published: 11 March 2013

Correspondence to: M. Boichu (m.boichu@lmd.polytechnique.fr)

Published by Copernicus Publications on behalf of the European Geosciences Union.

ACPD

13, 6553–6588, 2013

Inverting for volcanic SO₂ flux at high temporal resolution

M. Boichu et al.

Title Page

Abstract

Introduction

Conclusions

References

Tables

Figures



Back

Close

Full Screen / Esc

Printer-friendly Version

Interactive Discussion



Abstract

Depending on the magnitude of their eruptions, volcanoes impact the atmosphere at various temporal and spatial scales. The volcanic source remains a major unknown to rigorously assess these impacts. At the scale of an eruption, the limited knowledge of source parameters, including time-variations of erupted mass flux and emission profile, currently represents the greatest issue that limits the reliability of volcanic cloud forecasts. Today, a growing number of satellite and remote sensing observations of distant plumes are becoming available, bringing indirect information on these source terms. Here, we develop an inverse modeling approach combining satellite observations of the volcanic plume with an Eulerian regional chemistry-transport model (CHIMERE) to better characterise the volcanic SO₂ emissions during an eruptive crisis. The May 2010 eruption of Eyjafjallajökull is a perfect case-study to apply this method as the volcano emitted substantial amounts of SO₂ during more than a month. We take advantage of the SO₂ column amounts provided by a vast set of IASI (Infrared Atmospheric Sounding Interferometer) satellite images to reconstruct retrospectively the time-series of the mid-tropospheric SO₂ flux emitted by the volcano with a temporal resolution of ~ 2 h, spanning the period from 1 to 12 May 2010. The initialisation of chemistry-transport modelling with this reconstructed source allows for a reliable simulation of the evolution of the long-lived tropospheric SO₂ cloud over thousands of kilometres. Heterogeneities within the plume, which mainly result from the temporal variability of the emissions, are correctly tracked over a time scale of a week. The robustness of our approach is also demonstrated by the broad similarities between the SO₂ flux history determined by this study and the ash discharge behaviour estimated by other means during the phases of high explosive activity at Eyjafjallajökull in May 2010. Finally, we show how a sequential IASI data assimilation allows for a substantial improvement in the forecasts of the location and concentration of the plume compared to an approach assuming constant flux at the source. As the SO₂ flux is an important indicator of the volcanic activity, this approach is also of interest to monitor poorly instrumented volcanoes from space.

Inverting for volcanic SO₂ flux at high temporal resolution

M. Boichu et al.

Title Page

Abstract

Introduction

Conclusions

References

Tables

Figures



Back

Close

Full Screen / Esc

Printer-friendly Version

Interactive Discussion



1 Introduction

Volcanic degassing has a major effect on atmospheric chemistry and represents an important source of forcing of climate at various spatial and temporal scales (Robock and Oppenheimer, 2003; Mather, 2008; Oppenheimer et al., 2011). Among major volcanic gases, sulphur-rich emissions play a crucial role, as their conversion into long-lived micron-size sulfate aerosols impacts the climate in various ways. Until recently, it was conventionally admitted that only major eruptions would have a significant climatic effect, as they produce plumes able to quickly reach the tropopause and to penetrate the stratosphere where plume components cannot be washed out by precipitation (Robock, 2000). These large eruptions generate plumes rich in sulfate aerosols that can be transported and dispersed over a whole hemisphere within the course of a few weeks, screening solar radiation and cooling the atmosphere by some measurable amount (e.g. 0.6 °C over two-three years for Mount Pinatubo (Philippines) in 1991 (McCormick et al., 1995), a series of rigorous Northern Hemisphere winters after the Laki (Iceland) in 1783–84, Highwood and Stevenson, 2003). Within the stratosphere, volcanic aerosols also contribute to deplete ozone at mid and high latitudes (Solomon et al., 1998; Tabazadeh et al., 2002). This type of sporadic volcanic activity is one of the factors able to force climate variability with effects persisting from a few weeks to a few years according to the intensity, the duration and the location of the event. However, recent studies suggest that more frequent eruptions of lower magnitude (restricted to the low stratosphere) as well as persistent volcanic degassing in the troposphere may also significantly impact the radiative state of the atmosphere (Vernier et al., 2011; Schmidt et al., 2012). Consequently, studying volcanic gas emissions during eruptions, but also during periods of quiescent degassing, is of importance to assess the impact of volcanism as a whole on the atmosphere.

On the timescale of an eruption, knowledge of the volcanic source (e.g. gas mass flux, emission altitude/profile) is essential to simulate with reliability the atmospheric fate of the volcanic gas cloud (Webley and Mastin, 2009; Bonadonna et al., 2012).

ACPD

13, 6553–6588, 2013

Inverting for volcanic SO₂ flux at high temporal resolution

M. Boichu et al.

Title Page

Abstract

Introduction

Conclusions

References

Tables

Figures

◀

▶

◀

▶

Back

Close

Full Screen / Esc

Printer-friendly Version

Interactive Discussion



Inverting for volcanic SO₂ flux at high temporal resolution

M. Boichu et al.

Title Page

Abstract

Introduction

Conclusions

References

Tables

Figures

◀

▶

◀

▶

Back

Close

Full Screen / Esc

Printer-friendly Version

Interactive Discussion



During the eruption of a volcano monitored by an observatory, ground geophysical and geochemical measurements may help to estimate these parameters (Mastin et al., 2009; Petersen et al., 2012). However, only few volcanological observatories exist in comparison with the numerous active volcanoes worldwide. Moreover, major ash-rich explosive eruptions often lead to a malfunction or even complete loss of most ground instruments (Surono et al., 2012). In particular, the ash-rich plume may become opaque to ultra-violet radiations, leading to a failure of UV-DOAS (Ultra Violet Differential Optical Absorption Spectroscopy) methods, which are the only ground techniques allowing for a measurement of the gas flux (Oppenheimer, 2010; Galle et al., 2010). As an alternative to ground observations, recent advances in satellite remote sensing now provide images covering the full breadth of volcanic gas plumes at high spatial and temporal resolutions, which open new perspectives of reconstruction of the SO₂ flux (Carn and Bluth, 2003; Merucci et al., 2011). However, relating these observations, which consist in map views of vertically integrated plume concentration, to the gas flux released by the volcano, is a challenging task. Indeed, a description of the complex physical and chemical evolution of the plume from the source to the point of observation is required.

In this paper, we reconstruct the SO₂ flux history of the May 2010 Eyjafjallajökull eruption using an inverse modelling approach combining IASI infrared satellite imagery of the plume with the chemistry-transport Eulerian model CHIMERE. Compared to previous studies (Theys et al., 2013), the strength of our inverse modelling approach is that no a-priori knowledge of the volcanic SO₂ flux is required. While this eruption was fairly modest compared to historical Icelandic eruptions, such as the 1783–84 Laki eruption (Thordarson and Self, 2003), it was able to disrupt repeatedly air traffic over Europe, generating huge economical costs and losses (Harris et al., 2012). This eruption is a perfect case-study, as the volcano emitted substantial amounts of ash and SO₂ during more than a month. Our study focuses on the period extending from 1 to 12 May 2010, which corresponds to a phase of renewal of the explosive activity following a few days of relative quiescence (Gudmundsson et al., 2012). A remarkable series

Inverting for volcanic SO₂ flux at high temporal resolution

M. Boichu et al.

Title Page

Abstract

Introduction

Conclusions

References

Tables

Figures

◀

▶

◀

▶

Back

Close

Full Screen / Esc

Printer-friendly Version

Interactive Discussion



of IASI satellite observations, tracking the long-lived tropospheric SO₂ plume of Eyjafjallajökull over thousands of kilometers, is used in the inversion scheme to reconstruct the SO₂ flux released by the volcano with a high temporal resolution. The exploitation of these satellite observations is motivated by the fact that no instrument was installed on the ground at the time of the eruption that could allow for the continuous monitoring of gas emissions (Laursen, 2010).

In a first section, we describe the methodology. Then, we present time-series of the SO₂ emissions of Eyjafjallajökull in May 2010 deduced from retrospective assimilation of satellite observations. After assessing the robustness of this source reconstruction, we next show how its use for initialising chemistry-transport modelling allows for a consistent tracking of the volcanic SO₂ cloud, including heterogeneities within the plume which mainly result from the temporal variability of the emissions. We then discuss broad similarities between SO₂ and ash flux time-series at Eyjafjallajökull determined for the same period by Stohl et al. (2011). Finally, we show how a sequential assimilation of satellite observations yields a reliable forecast of the volcanic SO₂ plume over a time scale of a few days.

2 Methodology

2.1 Chemistry-transport model

CHIMERE is a state-of-the-art regional chemistry-transport model developed for studies of air quality (Rouil et al., 2009), transport of aerosols (Bessagnet et al., 2009), desert dust (Bessagnet et al., 2008) and recently volcanic plumes (Colette et al., 2011). Generally, this Eulerian model describes the physical and chemical processes affecting an emission during its transit in the atmosphere, including transport, turbulent mixing, diffusion, dry deposition, wet scavenging and gas/aqueous phase chemistry. For more details, the reader is referred to the online documentation of the CHIMERE model (CHIMERE, 2011). The model is driven in this study by meteorological forcing fields

Inverting for volcanic SO₂ flux at high temporal resolution

M. Boichu et al.

Title Page

Abstract

Introduction

Conclusions

References

Tables

Figures

◀

▶

◀

▶

Back

Close

Full Screen / Esc

Printer-friendly Version

Interactive Discussion



calculated using the mesoscale Weather Research and Forecast (WRF) model in its non-hydrostatic configuration. A horizontal 25 km × 25 km rectangular grid is defined over a large domain extending North-South from Greenland to North Africa, and West-East from North America East Coast to Eastern Europe. The model includes here 18 vertical levels extending up to 200 hPa. The vertical grid is a hybrid sigma-pressure coordinate system in the lower troposphere, until the altitude at which the difference of pressure between two consecutive levels in this hybrid coordinate system exceeds 50 hPa. Above this altitude, levels are equally spaced in terms of pressure, with a spacing fixed to 50 hPa, to allow for a higher vertical resolution in the mid/upper troposphere where the Eyjafjallajökull plume traveled in May 2010. SO₂ emissions are released along a 1 km-FWHM semi-Gaussian profile, centered at a height of 6 km a.s.l. in agreement with C-band radar and web cameras observations of the altitude of Eyjafjallajökull emissions over the 4–12 May 2010 period (Petersen et al., 2012). The long lifetime (about a week) of the tropospheric plume of Eyjafjallajökull during the studied period of time indicates that the loss of SO₂ was very slow. Therefore, for the sake of simplicity, removal mechanisms of SO₂ (dry/wet deposition and SO₂ oxidation), which are more-over poorly-constrained for tropospheric volcanic plumes (Oppenheimer et al., 1998; Delmelle, 2003), were not included in the modelling. As shown in Sect. 3.2, despite this simplification, a satisfactory agreement is reached between plume simulations and observations in terms of the decrease of the SO₂ column amount as a function of plume age.

2.2 Satellite observations

The Infrared Atmospheric Sounding Interferometer (IASI) carried on board the polar-orbiting MetOp-A satellite provides since 2006 global coverage of the atmospheric composition twice a day (overpass at ~09:30 and 21:30 LT at Equator) in the nadir geometry (polar sun-synchronous), with a footprint of 12 km diameter (at nadir) and full swath width of 2200 km (Clerbaux et al., 2009). The Fourier Transform spectrometer spans a spectral range from 645 to 2760 cm⁻¹ with no gaps, an apodized resolution of

0.5 cm⁻¹ and a sampling of 0.25 cm⁻¹. It consequently covers three bands of SO₂ absorption in the mid-infrared. Here we use the IASI SO₂ product described in Clarisse et al. (2012). It is based on brightness temperature differences (BTD) and relies on lookup tables for the conversion of temperatures to SO₂ total columns. The retrieval algorithm was designed for plumes above the lower troposphere (~ 5 km) where it has a low theoretical uncertainty (~ 5%). The largest uncertainties in the product are due to plume altitude, which is not retrieved but assumed and fixed to a constant value. Various plume altitudes were tested, covering values close to the emission height, which varied around 6 km a.s.l in the first weeks of May 2010 (Petersen et al., 2012). For a 5 km altitude, the retrieval algorithm regularly fails to converge in the region close to Iceland, although BTD anomalies suggest the presence of the SO₂ plume. This may be due to an under-estimation of the actual altitude of the plume, the presence of thick overlaying meteorological clouds or the influence of a strong ash load in the plume. Assuming a 7 km altitude, the plume extent is well restituted by the retrieval analysis, in agreement with anomalies in BTD. For the sake of stability of the retrieval outputs, we consequently assume a plume altitude of 7 km a.s.l. To reduce the impact of the noise, observations with a BTD smaller than 0.3 K were assumed to have a zero SO₂ column. This threshold corresponds to a SO₂ column amount of ~ 0.5 DU, according to the linear correlation observed between weak values of SO₂ BTD and total column amounts. Retrieved NaN values of column amounts, which result from occasional failure of the algorithm to converge, are disregarded in the further data analysis.

2.3 Inversion scheme

We adopt an inverse modelling approach to reconstruct the volcano SO₂ emissions using satellite observations of the plume and a chemistry-transport model. In the discrete forward problem, the observed SO₂ column amounts (d) are a function (g) of the SO₂ flux released by the volcano as a function of time (m)

$$d = g(m). \quad (1)$$

Inverting for volcanic SO₂ flux at high temporal resolution

M. Boichu et al.

Title Page

Abstract

Introduction

Conclusions

References

Tables

Figures

⏪

⏩

◀

▶

Back

Close

Full Screen / Esc

Printer-friendly Version

Interactive Discussion



The function g describes the physical and chemical processes affecting a parcel of SO_2 travelling from the volcano vent to the observation point. This problem can be considered linear as it is resolved given a prescribed meteorological field, with processes of transport, diffusion and deposition affecting linearly a given emission flux. Therefore,

Eq. (1) can be written in matrix form: $\mathbf{d} = \mathbf{G}\mathbf{m}$, where \mathbf{d} and \mathbf{m} represent vectors of data and model parameters. This means that we can find a linear combination of source elements \mathbf{m} whose projection into the data space matches best the satellite observations in \mathbf{d} . Some minor effects, such as the detection limit of satellite observations, imply nevertheless a weak non-linearity. The vector \mathbf{m} is discretised with a 1 h timestep, as meteorological data are provided on a hourly basis. \mathbf{G} represents the forward operator whose values are calculated using the CHIMERE model (Sect. 2.1) on the grid of IASI observations (Sect. 2.2) which depends on latitude, longitude and time.

Looking for a smoothed SO_2 flux solution, we seek the model parameters $\hat{\mathbf{m}}$ that minimise both the L_2 norm of the misfit function $(\mathbf{d} - \mathbf{G}\mathbf{m})$ (Tarantola, 2005) and the second derivative of \mathbf{m} (e.g. Jonsson, 2002). This modifies the system of equations as follows

$$\begin{bmatrix} \mathbf{d} \\ 0 \end{bmatrix} = \begin{bmatrix} \mathbf{G} \\ K^2 \Delta \end{bmatrix} \times \mathbf{m} \quad (2)$$

where Δ represents the discrete Laplace operator and K^2 the Lagrange multiplier which characterises the degree of smoothing. Since a relevant physical value for the SO_2 flux is necessarily positive, an additional constraint of non-negativity of the solution is applied (Lawson and Hanson, 1974). No a-priori on the solution is assumed in the inversion procedure, as knowledge of the volcanic SO_2 source is generally very poor, if not nonexistent.

K^2 is not an adequate quantity to determine the degree of smoothing adapted to the solution, as it depends on the number of data. Therefore, a new quantity is defined, the

Inverting for volcanic SO_2 flux at high temporal resolution

M. Boichu et al.

Title Page

Abstract

Introduction

Conclusions

References

Tables

Figures

◀

▶

◀

▶

Back

Close

Full Screen / Esc

Printer-friendly Version

Interactive Discussion



solution roughness ρ , which represents the average discrete second derivative of \hat{m} :

$$\rho = \frac{\sum_{i=1}^N |\rho_i|}{N}, \quad (3)$$

with $\rho = \Delta \hat{m}$ and N the number of SO₂ flux values. Figure 1 shows how the fit to observations decreases significantly for roughness values $< 90 \text{ ton hour}^{-3}$. However, the misfit remains constant for roughness exceeding a value of $100 \text{ ton hour}^{-3}$, which is consequently chosen as the optimal roughness in our inversion procedure. The magnitude of the smoothing constraint controls the spread in time (and hence in space) of any given emission peak. As a consequence, peak values of the reconstructed SO₂ flux depend on the amount of smoothing, whereas the total mass of the emissions (integral of the flux history) should be less sensitive to this parameter.

In a first attempt, we have performed an inversion using all the available observations in a satellite image. However, the plume intensity modeled according to this procedure generally appears to be under-estimated (Fig. 2a). Three reasons explain this discrepancy. First, a small shift in space between modeled and observed plumes may occur, owing to imperfections in the reanalysed meteorological fields (Fig. 3a). The error on the modeled plume location generally increases when the plume gets older, as errors on meteorological variables tend to accumulate with time. Secondly, the numerical diffusion inherent to Eulerian models leads to an over-estimation of plume dispersion (Fig. 3b). Thirdly, given the low altitude of the Eyjafjallajökull plume in May 2010, parts of the plume may be missed by satellite observations on numerous occasions as they generate a signal lower than the detection limit (Fig. 3c). Consequently, null observations should not be systematically interpreted as indications of the actual absence of the plume. Due to the combination of these three phenomena, numerous null observations (i.e. no plume detection) are illegitimately accounted for in the inversion algorithm, resulting in an under-estimation of the plume intensity. To circumvent this issue, we perform a decimation of the numerous observations indicating an absence of the plume. As shown in Fig. 2b, the decimation of null data yields a more accurate

Inverting for volcanic SO₂ flux at high temporal resolution

M. Boichu et al.

Title Page

Abstract

Introduction

Conclusions

References

Tables

Figures

◀

▶

◀

▶

Back

Close

Full Screen / Esc

Printer-friendly Version

Interactive Discussion



Inverting for volcanic SO₂ flux at high temporal resolution

M. Boichu et al.

Title Page

Abstract

Introduction

Conclusions

References

Tables

Figures

◀

▶

◀

▶

Back

Close

Full Screen / Esc

Printer-friendly Version

Interactive Discussion



modelling of the plume intensity. Naturally, the degree of data decimation is bound to impact on the reconstructed SO₂ flux history. As less null data points are kept, the misfit in regions where the model cannot reproduce an apparent absence of SO₂ (especially near plume edges or in aged parts of the plume) tends to weight less significantly in the overall misfit. Therefore, the magnitude of the reconstructed emissions should increase as the strength of null data decimation. However, an excessive reduction of the number of null observations kept in the inversion degrades the quality of the simulation by enhancing the spreading of the plume (Fig. 2c). Here, as a compromise between an excessive plume spreading and an obviously under-estimated SO₂ flux, we choose to keep one out of ten null data points, chosen randomly (Fig. 2b). An additional advantage of the data decimation is the considerable reduction of the size of the matrices to invert, which allows for the assimilation of long time-series of observations.

Under specific meteorological conditions, old parts of the plume may overlap with younger parts, as observed during the Eyjafjallajökull eruption in May 2010. To avoid the ambiguities in the source reconstruction resulting from this effect, plume parts older than 3.5 days are not accounted for in the inversion algorithm but are kept for plume simulations. Although relatively ineffective when observations originate from a single image, this selection process significantly improves the quality of the reconstruction when several observations of any given gas parcel are available, as relatively young plume parts are the best simulated in terms of accuracy on plume location and intensity, for the reasons mentioned earlier.

In the following, we will apply the above-described assimilation procedure to either a single satellite image, or to a set of several images. These two procedures will be named “single-” or “multiple-image” inversion, respectively.

2.4 Main sources of uncertainty

2.4.1 IASI retrieval

Several factors may influence the SO₂ column amounts retrieved from IASI observations, with impacts on the estimated volcanic gas flux. For instance, gaps in satellite images, due to interruptions in satellite data transmission or the presence of thick meteorological clouds masking any underlying SO₂ plume, may lead to a local underestimation of the SO₂ concentration, and hence errors in the reconstructed SO₂ flux history. However, the short revisit time of IASI (~ 12 h at Equator, less at higher altitudes thanks to overlapping satellite tracks) allows for redundant observations of a given SO₂ parcel during its lifetime as it transits through the atmosphere. Although critical for a single-image inversion, the sensitivity to gaps in the spatial coverage of the volcanic plume is expected to decrease significantly in a multiple-image inversion.

Another important issue is the SO₂ detection level of IASI satellite observations, which depends on both the instrument and the retrieval algorithm. Currently, the minimum SO₂ column amount detectable from space restricts the analysis of volcanic degassing to eruptive phases where a significant mass of SO₂ is expelled from the volcano. Our analysis suggests that a minimum SO₂ flux of ~ 1 kg s⁻¹ is required to exceed the IASI SO₂ detection threshold in the dispersed Eyjafjallajökull plume. However, this value is specific to the case studied here, and should vary from one eruption to another, depending mainly on meteorological conditions, plume altitude and latitude, which all impact the IASI retrieval. Generally, detection of the plume will be facilitated by low humidity and emission at high altitude, which favour a longer lifetime of the SO₂ plume (Graf et al., 1997), as well as low wind speed leading to a slower dispersion of the plume. Since the IASI SO₂ retrieval algorithm used here has limited sensitivity below ~ 5 km due to competing water absorption (Clarisse et al., 2012), lower tropospheric SO₂ emissions, which often correspond to low levels of degassing, cannot be detected.

Retrieved IASI SO₂ abundances may also be affected by the concomitant existence in the volcanic cloud of various particles, including ash, ice and sulfate aerosols. All these absorb infrared radiations in the spectral window used for the SO₂ retrieval. A significant overestimation (up to 50 %) of the SO₂ abundance is expected with a high load in ash or aerosols, if the plume is not completely obscured by their presence (Clarisse et al., 2012).

2.4.2 Emission height and plume altitude

Volcanic gases generally tend to rise up to a certain altitude above the source, named here the emission height, prior to being transported and dispersed by atmospheric circulation. For the case of weak emissions, the associated plume may be bent by local wind (Oddsson et al., 2012). More generally, emission height depends on several parameters, including the composition and temperature of the erupting mixture, the mass eruption rate, the volcano latitude and altitude, and the local meteorological field (Sparks et al., 1997).

The influence of emission height on retrieved volcanic flux is twofold. First, the emission height plays a role in the plume simulation, as volcanic gas is introduced in the numerical grid within a certain range of pressure levels. Depending on meteorological conditions, horizontal shearing within the atmospheric column may lead to significant differences in the subsequent trajectory of gas parcels emitted at a given location but different altitudes. Therefore, if emission height is initialised incorrectly, a possible divergence between observed and modeled SO₂ maps with increasing plume age may occur. On the other hand, in case of a poor knowledge of the emission height, one could determine the most likely emission height by comparing the predicted plume trajectory with the actual distribution of gas parcels imaged by satellite imagery using inverse modelling approaches (Eckhardt et al., 2008; Kristiansen et al., 2010; Krotkov et al., 2010). Following this strategy requires considering that the meteorological field is known with good confidence. In the specific case of the Eyjafjallajökull plume of May 2010, no significant divergence in predicted plume trajectories could be found

Inverting for volcanic SO₂ flux at high temporal resolution

M. Boichu et al.

Title Page

Abstract

Introduction

Conclusions

References

Tables

Figures



Back

Close

Full Screen / Esc

Printer-friendly Version

Interactive Discussion



among the different emission heights that have been tested (4 to 8 km). This suggests that the errors on emission trajectory resulting from uncertainty on emission height only produce modest errors on the reconstructed SO₂ flux history.

The emission height also conditions the altitude of the plume at distance from the volcano. In order to convert the brightness temperature collected by IASI into a SO₂ column amount, an assumption on the plume altitude, which is assumed constant in our retrieval algorithm, is necessary (Sect. 2.2). Since the sensitivity to SO₂ decreases below ~ 10 km with the algorithm used here, the retrieved IASI SO₂ concentration depends strongly on the assumed plume elevation. Typically, for a given brightness temperature in our study, decreasing the assumed plume altitude from 10 km to 7 km, or from 7 km and to 5 km increases the retrieved SO₂ column amount by a factor of ~ 2 or ~ 3, respectively. Consequently, an uncertainty on the absolute value of the reconstructed SO₂ flux may arise from poor knowledge of the plume altitude. Nevertheless, the emission height did not vary significantly during the course of the 2010 May eruption (Petersen et al., 2012). Since the plume altitude is expected to follow a similar behaviour, relative variations of the SO₂ flux should remain a robust feature of the inversion results.

3 Results and discussion

3.1 Robustness of the source reconstruction explored through single- versus multiple-image inversion

In Fig. 4, we show the reconstructed SO₂ emissions deduced from the thirteen maps of SO₂ column amounts derived from available IASI observations, which cover the period 1 May p.m.–12 May a.m. During this period, IASI always detects the Eyjafjallajökull SO₂ plume except on 1 May p.m. and 2 May a.m., in agreement with the recorded low level of volcanic activity characterised by low effusive magma discharge (Gudmundsson et al., 2012). Time-series *a* to *m* displayed in Fig. 4 correspond to the inversion of

Inverting for volcanic SO₂ flux at high temporal resolution

M. Boichu et al.

Title Page

Abstract

Introduction

Conclusions

References

Tables

Figures

◀

▶

◀

▶

Back

Close

Full Screen / Esc

Printer-friendly Version

Interactive Discussion



Inverting for volcanic SO₂ flux at high temporal resolution

M. Boichu et al.

Title Page

Abstract

Introduction

Conclusions

References

Tables

Figures

◀

▶

◀

▶

Back

Close

Full Screen / Esc

Printer-friendly Version

Interactive Discussion



single maps, i.e. independently of each other (“single-image inversion”). Strong temporal variations of the SO₂ flux are apparent in these time-series. Observations span the period from 1 to 12 May, but no SO₂ emissions can be detected prior to 4 May. From 4 to 12 May, short and recurrent periods of intense degassing (3–7 h) are followed by longer intervals of weak degassing. The time and amplitude of SO₂ peaks are remarkably consistent among the different and independent inversions (Fig. 4). This confirms that heterogeneities observed within the plume by IASI can be mainly explained by temporal variations of the volcanic degassing at the source. Thanks to the short revisit time of IASI, SO₂ released during a given event of degassing is captured multiple times during its transit through the atmosphere (Fig. 5). Our inversion procedure allows us to associate regions of relatively higher SO₂ concentrations in IASI maps to individual peaks of SO₂ emissions at the source.

Nevertheless, minor differences among SO₂ flux time series reconstructed from single-image inversions can be observed. The amplitude of most SO₂ peaks, as well as the SO₂ mass expelled during the associated degassing event, vary by a factor of ~2. The peak time-locations vary on a maximum range of 2 h around the central peak location, which provides a rough estimate of the time-resolution of the reconstructed SO₂ flux time-series. Part of this variability is due to the fact that the single-image inversion suffers from an increase of the uncertainty on the SO₂ emissions as plume age increases. Moreover, a few artifactual degassing events can also be observed, as illustrated by the SO₂ peak appearing on 6 May at 20:00 UTC in the flux time-series retrieved from an IASI image acquired on 10 May (Fig. 4, i). This spurious peak is deduced from a ~3.5 day old plume which is close to the age limit chosen in Sect. 2.3 to select observations taken into account in the inversion scheme. The error on the timing of the emission associated with this peak results from the difficulty of deducing valuable information on the source from the observation of the older part of the plume. For this case, the residual SO₂ column amount anomaly appears spread and uniform as a result of dispersion and shearing of the plume during its atmospheric transit.

Inverting for volcanic SO₂ flux at high temporal resolution

M. Boichu et al.

Title Page

Abstract

Introduction

Conclusions

References

Tables

Figures

◀

▶

◀

▶

Back

Close

Full Screen / Esc

Printer-friendly Version

Interactive Discussion



To avoid these shortcomings, we assimilate the full set of available satellite observations into a multiple-image inversion procedure (Fig. 4, *). This approach allows for the retrieval of SO₂ emissions with a higher accuracy on intensity and an improved temporal resolution. The reconstructed SO₂ emissions span the full period of available IASI observations (1 May p.m.–12 May a.m.). Despite an uneven sampling in time due to a few missing acquisitions (2 May p.m., 3 May, 4 May a.m., 5 May a.m., 6 May, incomplete map for 8 May a.m.), the resolution appears to be relatively uniform. From the comparison of the flux histories derived from single- and multiple-image inversions (Fig. 4), we observe that more weight is attributed in the multiple-image inversion scheme to observations of young plume parts. Young parcels are generally the densest in SO₂, which gives them a significant role for minimising the overall residual of the fit to data in the inversion scheme. Since both errors on meteorological data and over-estimation of modeled dispersion increase with plume age, the location and the intensity of young SO₂ parcels are modeled with a better accuracy than older parts of plume. Therefore, multiple-image inversion allows to pool the observations of young plume parts from each single image to provide a more accurate reconstructed source.

3.2 Linking in-plume heterogeneities to the temporal variability of the volcanic source

In Fig. 5, we show selected maps of observed and modeled SO₂ column amounts from the multiple-image inversion. The complete time-series of plume maps is available in Appendix A1, A2 (Figs. A1 and A2). At least nine well defined peaks of SO₂ emission are deduced from the time-series inversion. This highlights the strong variability of volcanic emissions during the Eyjafjallajökull May 2010 eruption. The strongest peaks correspond to spatially separated SO₂ parcels that can be tracked for up to 6 days after their emission, which represents a long lifetime for tropospheric SO₂. After 6 days, these old SO₂ puffs generally disappear from the maps as their intensity decreases below IASI detection threshold. We are also able to reproduce the entrainment of the plume in a large vortex over the Atlantic Ocean, leading to considerable shearing and

5 mixing of SO₂ emissions (e.g. Fig. 5f–h). Moreover, due to the specific meteorological field that prevailed at the time of the eruption, SO₂ emissions released on 5–6 May are transported back to Iceland after a long travel of several thousands of kilometers and overlap with younger emissions around 10 May (Fig. 5g and h). Thanks to the criterion establishing a threshold on the age of modeled emissions used in the inversion (Sect. 2.3), we are able to rigorously reconstruct the source by discriminating between older and younger emissions. Despite the over-estimation of plume dispersion inherent to Eulerian models (linked to numerical diffusion), the location, spatial extent and intensity of the simulated volcanic cloud using the reconstructed source is in strong agreement with observations. These various lines of evidence demonstrate the robustness of the approach used in this study to refine our ability to model the fate of volcanic plumes.

3.3 Comparison of the temporal evolutions of SO₂ versus ash fluxes

15 No ground techniques allowing for the continuous monitoring of gas emissions were operational on Eyjafjallajökull during its 2010 eruption (Laursen, 2010). In contrast, the significant release of ash, which is another major component of volcanic emissions during explosive eruptions, was studied in details (Gudmundsson et al., 2012; Stohl et al., 2011). Both SO₂ and ash carry important information on the volcanic activity. The monitoring of SO₂ provides clues on various processes and variables, including stored/ascending magma volumes, depth of magma/volatile storage, edifice and magma permeability, and the influence of the hydrothermal system (Oppenheimer et al., 2003; Edmonds, 2008). On the other hand, ash discharge informs on the degree of magma fragmentation at shallow depth and eruptive explosivity (Cashman et al., 2000). During any explosive eruptive episode, both SO₂ and ash releases generally
25 tend to broadly follow the same trend. However, departure from a simple parallel evolution of SO₂ and ash discharge might occur in certain circumstances, such as during the transitions between successive eruptive regimes (e.g. Andronico et al., 2009). The comparison of ash and SO₂ release rates is consequently of interest to assess the

Inverting for volcanic SO₂ flux at high temporal resolution

M. Boichu et al.

Title Page

Abstract

Introduction

Conclusions

References

Tables

Figures



Back

Close

Full Screen / Esc

Printer-friendly Version

Interactive Discussion



validity of our SO₂ source reconstruction but also to explore the underlying magma dynamics driving the eruption.

Figure 6 shows the temporal evolution of Eyjafjallajökull SO₂ degassing determined by this study and the ash release rate estimated by Stohl et al. (2011). These authors developed an inverse modelling approach to reconstruct the altitude and the rate of ash emissions at Eyjafjallajökull, combining ash satellite observations (from SEVIRI and IASI) with the Lagrangian particle dispersion model FLEXPART. Broad similarities are observed between the two time-series, with major episodes of ash and SO₂ discharge detected quasi-simultaneously in the period 6–12 May, and low emissions before 4 May. From 6 to 8 May included, amplitudes of ash and SO₂ peaks, relatively to the baseline estimated respectively at $\sim 1 \text{ ts}^{-1}$ and $\sim 0.1 \text{ kth}^{-1}$ from 1 to 3 May, are in agreement. Episodes of SO₂ degassing are nevertheless of shorter duration than concurrent ash release events, possibly owing to the higher time-resolution of the inversion procedure developed in the present study. This strong similarity illustrates the robustness of the SO₂ source reconstruction.

Nevertheless, some discrepancies are also noticed. Uncertainties associated with inversion procedures, including errors on the retrieval of satellite observations and on plume modelling, may explain this discrepancy. Depending on the style of eruptive activity, we also expect SO₂ and ash releases to exhibit a distinct behaviour. From 9 to 12 May, SO₂ emissions are relatively twice weaker than ash, with average SO₂ and ash emission rates respectively in excess within a factor 3 and 6 of baseline values. A constant plume altitude of 7 km is assumed in the IASI retrieval whereas emission height seems to progressively decrease down to ~ 4 km from 8 to 12 May according to combined radar and web camera observations (Petersen et al., 2012). By comparing outputs from IASI retrieval assuming two different Eyjafjallajökull plume altitudes of 5 and 7 km (IASI being almost insensitive to emissions < 5 km), we observe variations of SO₂ column amounts within a factor 2–3. Therefore, this assumed over-estimated plume height may lead to an under-estimation of the same order of the SO₂ flux at

Inverting for volcanic SO₂ flux at high temporal resolution

M. Boichu et al.

Title Page

Abstract

Introduction

Conclusions

References

Tables

Figures

◀

▶

◀

▶

Back

Close

Full Screen / Esc

Printer-friendly Version

Interactive Discussion



source reconstructed by inversion, and could explain the factor ~ 2 observed between ash and SO_2 emission rates.

However, errors on plume altitude cannot be invoked to explain the strikingly different behaviours of SO_2 and ash discharge on 4 and 5 May. After several days of low volcanic activity, an intense degassing episode (peaking at $\sim 0.4 \text{ kth}^{-1}$) is recorded on 4 May a.m., a few hours before an ash release event reaching $\sim 2 \text{ ts}^{-1}$. It is followed by a few hours of low SO_2 degassing (under the detection level) before an abrupt and significant SO_2 release of $\sim 0.7 \text{ kth}^{-1}$ in the early hours of 5 May, which coincides with weak ash emissions. Strong values of the SO_2 flux, increasing between 0.15 and 0.8 kth^{-1} , are also recorded on 5 May p.m., followed by a few hours of quiescence preceding the largest SO_2 degassing episode for the studied period, which peaks on 6 May around 8 a.m. at 2.1 kth^{-1} . The behaviour of ash discharge is different, with weak emissions until the end of 5 May, and a more or less abrupt increase (depending on the meteorological field used to force the simulation) culminating on 6 May with the major ash event of the period characterised by a rate of $\sim 20 \text{ ts}^{-1}$. These different release behaviours of ash and SO_2 could be compatible with processes of gas/melt separation in the volcanic edifice in the days preceding the major explosive phase on 6 May (Gonnermann and Manga, 2007; Edmonds, 2008).

3.4 Forecasting volcanic plume evolution

The stability of the source reconstructed retrospectively through single-map inversions demonstrates that the transit of in-plume heterogeneities through the atmosphere can be modeled reliably over a time scale of several days (Fig. 4). This result suggests that forecasting the fate of the volcanic cloud could be readily achieved by sequential data assimilation. Figure 7 shows a comparison between, on one hand, the forecasts initialised using the source reconstructed by the inversion of the 7 May 2010 image, and, on the other hand, independent images acquired on 9 and 10 May 2010 (+2 days and +3 days respectively). This simulation mimics the situation that could prevail at the

Inverting for volcanic SO_2 flux at high temporal resolution

M. Boichu et al.

Title Page

Abstract

Introduction

Conclusions

References

Tables

Figures

◀

▶

◀

▶

Back

Close

Full Screen / Esc

Printer-friendly Version

Interactive Discussion



Inverting for volcanic SO₂ flux at high temporal resolution

M. Boichu et al.

Title Page

Abstract

Introduction

Conclusions

References

Tables

Figures

◀

▶

◀

▶

Back

Close

Full Screen / Esc

Printer-friendly Version

Interactive Discussion



beginning of a volcanic crisis, when only one image of the plume would be available in the few hours following the inception of the eruption. The entrainment of the plume in the Atlantic vortex at +2 days is correctly described, although a slight advance of the modeled plume front can be noticed. A broad agreement between model and data is reached with the forecast at +3 days, including the appropriate description of an elongated old part of the plume over thousands of kilometres from North Africa to Iceland. Nevertheless, we note some shift between the location of the modeled and observed plume fronts, due to the slight error on plume front location already visible on the previous day. The CHIMERE model is forced here by re-analysed WRF meteorological fields. We consequently do not expect the same degree of agreement for a near real-time analysis, where only prognostic meteorological fields would be available. Other differences between observations and simulations are not linked to the quality of the forecast but rather result from the renewed discharge of SO₂ by Eyjafjallajökull on 8 and 9 May, which mixes in the atmosphere with older emissions. Alternatively, assuming a constant SO₂ flux in the time interval following the last satellite observation could help to achieve a more conservative forecast. In the near future, significant improvements in the reliability of volcanic plume forecasts will likely be achieved thanks to the planned acceleration of revisit time and increased sensitivity of future spaceborne gas sounders (Veefkind et al., 2012; Clerbaux and Crevoisier, 2013), as well as ever-advancing progress in operational meteorology.

4 Conclusions and perspectives

This paper illustrates how a simple inversion procedure combining IASI satellite observations and the chemistry-transport model CHIMERE permits to retrospectively reconstruct the SO₂ flux history at Eyjafjallajökull in May 2010 with a temporal resolution of ~2 h. This method could more generally be developed with any satellite product. In this approach, the synergy of short revisit-time satellite observations and accurate modeling of atmospheric dynamics make a-priori assumptions on the emissions

Inverting for volcanic SO₂ flux at high temporal resolution

M. Boichu et al.

Title Page

Abstract

Introduction

Conclusions

References

Tables

Figures

◀

▶

◀

▶

Back

Close

Full Screen / Esc

Printer-friendly Version

Interactive Discussion



unnecessary. This is a major advantage when little information is available on the volcanic source, which is generally the case. The stability of the source reconstructed by single- or multiple-image inversions demonstrates the robustness of the method, as well as the agreement over the time scale of a few days between observed and modeled location, extent and internal structures of the volcanic SO₂ cloud. The broad similarity between SO₂ (this study) and ash (Stohl et al., 2011) emissions also supports the consistency of the retrieved SO₂ source.

As SO₂ represents an important indicator for the volcanic activity, the reconstruction of the volcanic SO₂ flux from spaceborne data assimilation opens new perspectives for the monitoring of poorly-instrumented volcanoes. Nevertheless, only ground-based methods relying on UV Differential Optical Absorption Spectroscopy are currently sensitive enough to estimate the low SO₂ fluxes that characterise pre-eruptive phases. However, these methods reach their effective limit during explosive phases. In such conditions, even if the ground installations have been spared by the eruption, the ash-rich plume may become opaque to UV, leading to a failure of spectroscopic methods. Moreover, in contrast to IR satellite imagery, UV spectroscopic methods do not operate during night-time. Therefore, gathering both ground-based and spaceborne UV/IR SO₂ measurements is crucial to continuously monitor the volcanic SO₂ flux from quiescent through to eruptive periods. This study opens the path for such developments in the near future.

No ground instruments were installed on Eyjafjallajökull, at the time of the 2010 eruption, for monitoring gas emissions. Consequently, the reconstructed bi-hourly resolved time-series of the SO₂ flux presented in this paper brings new information on the volcanic and magmatic activities at Eyjafjallajökull in May 2010. Coupling these new geochemical data with available geophysical and petrological observations should make possible to re-investigate the processes responsible for changes in the volcanic behaviour observed during this eruptive phase.

SO₂ satellite observations are often used to perform ash plume forecasts, as SO₂ is generally considered as a good proxy for the presence of ash in a volcanic cloud.

However, whereas the two species are generally co-located in the volcanic cloud, they can sometimes follow separate trajectories in the atmosphere. If such an event is not detected, it may represent a considerable hazard for air traffic. In this paper, we show that the proposed inversion method, once implemented in a sequential data assimilation mode, could help to improve the reliability of delivered forecasts of SO₂ volcanic plumes. Little would be required to develop a similar inversion approach for reconstructing ash emissions in order to carry out a combined analysis of SO₂ and ash plumes, which is the best method to rigorously follow the fate of a volcanic plume in the atmosphere.

Acknowledgements. We gratefully acknowledge support from the French ANR funded CHEDAR project. MB warmly thanks Jean-Luc Got (ISTerre) for fruitful discussions on inverse modelling, Philippe Drobinski and Palmira Messina (LSCE) for helpful discussions. IASI has been developed and built under the responsibility of the Centre National d'Etudes Spatiales (CNES, France). It is flown onboard the Metop satellites as part of the EUMETSAT Polar System. The IASI L1 data are received through the EUMETCast near real time data distribution service. L. Clarisse is a Postdoctoral Researcher (Chargé de Recherches) with F.R.S.-FNRS. C. Clerbaux is grateful to CNES for scientific collaboration and financial support. The research in Belgium was funded by the F.R.S.-FNRS (M.I.S. nF.4511.08), the Belgian State Federal Office for Scientific, Technical and Cultural Affairs and the European Space Agency (ESA-Prodex arrangements and the Support to Aviation Control Service (SACS+) project). We also acknowledge financial support from the EVOSS project (2nd Space Call of the 7th Framework Program of the European Commission, with grant agreement 242535) and the "Actions de Recherche Concertées" (Communauté Française de Belgique).



The publication of this article is financed by CNRS-INSU.

6574

ACPD

13, 6553–6588, 2013

Inverting for volcanic SO₂ flux at high temporal resolution

M. Boichu et al.

Title Page

Abstract

Introduction

Conclusions

References

Tables

Figures

⏪

⏩

◀

▶

Back

Close

Full Screen / Esc

Printer-friendly Version

Interactive Discussion



References

- Andronico, D., Cristaldi, A., Del Carlo, P., and Taddeucci, J.: Shifting styles of basaltic explosive activity during the 2002–03 eruption of Mt. Etna, Italy, *J. Volcanol. Geoth. Res.*, 180, 110–122, doi:10.1016/j.jvolgeores.2008.07.026, 2009. 6569
- 5 Bessagnet, B., Menut, L., Aymoz, G., Chepfer, H., and Vautard, R.: Modeling dust emissions and transport within Europe: the Ukraine March 2007 event, *J. Geophys. Res.*, 113, D15202, doi:10.1029/2007JD009541, 2008. 6558
- Bessagnet, B., Menut, L., Curci, G., Hodzic, A., Guillaume, B., Lioussé, C., Moukhtar, S., Pun, B., Seigneur, C., and Schulz, M.: Regional modeling of carbonaceous aerosols over Europe – focus on secondary organic aerosols, *J. Atmos. Chem.*, 61, 175–202, 2009. 6558
- 10 Bonadonna, C., Folch, A., Loughlin, S., and Puempel, H.: Future developments in modelling and monitoring of volcanic ash clouds: outcomes from the first IAVCEI-WMO workshop on Ash Dispersal Forecast and Civil Aviation, *Bull. Volcanol.*, 74, 1–10, doi:10.1007/s00445-011-0508-6, 2012. 6556
- 15 Carn, S. A. and Bluth, G. J. S.: Prodigious sulfur dioxide emissions from Nyamuragira volcano, D. R. Congo, *Geophys. Res. Lett.*, 30, 2211, doi:10.1029/2003GL018465, 2003. 6557
- Cashman, K., Sturtevant, B., Papale, P., and Navon, O.: Magmatic fragmentation, in: *Encyclopedia of Volcanoes*, 421–430, Academic Press, 2000. 6569
- CHIMERE: Documentation of the Chemistry-Transport Model CHIMERE, Tech. Report, CNRS, IPSL, INERIS, available at: <http://www.lmd.polytechnique.fr/chimere>, 2011. 6558
- 20 Clarisse, L., Hurtmans, D., Clerbaux, C., Hadji-Lazaro, J., Ngadi, Y., and Coheur, P.-F.: Retrieval of sulphur dioxide from the infrared atmospheric sounding interferometer (IASI), *Atmos. Meas. Tech.*, 5, 581–594, doi:10.5194/amt-5-581-2012, 2012. 6560, 6564, 6565
- Clerbaux, C. and Crevoisier, C.: New directions – infrared remote sensing of the troposphere from satellite: less, but better, *Atmos. Environ.*, submitted, 2013. 6572
- 25 Clerbaux, C., Boynard, A., Clarisse, L., George, M., Hadji-Lazaro, J., Herbin, H., Hurtmans, D., Pommier, M., Razavi, A., Turquety, S., Wespes, C., and Coheur, P.-F.: Monitoring of atmospheric composition using the thermal infrared IASI/MetOp sounder, *Atmos. Chem. Phys.*, 9, 6041–6054, doi:10.5194/acp-9-6041-2009, 2009. 6559
- 30 Colette, A., Favez, O., Meleux, F., Chiappini, L., Haefelin, M., Morille, Y., Malherbe, L., Papin, A., Bessagnet, B., Menut, L., Leoz, M., and Rouil, L.: Assessing in near real time the impact of

Inverting for volcanic SO₂ flux at high temporal resolution

M. Boichu et al.

Title Page

Abstract

Introduction

Conclusions

References

Tables

Figures

◀

▶

◀

▶

Back

Close

Full Screen / Esc

Printer-friendly Version

Interactive Discussion



the April 2010 Eyjafjallajökull ash plume on air quality, *Atmos. Environ.*, 45, 1217–1221, doi:10.1016/j.atmosenv.2010.09.064, 2011. 6558

Delmelle, P.: Environmental impacts of tropospheric volcanic gas plumes, in: *Volcanic Degassing*, edited by: Oppenheimer, C., Pyle, D. M., and Barclay, J., *Geol. Soc. Spec. Publ.*, 213, 381–400, 2003. 6559

Eckhardt, S., Prata, A. J., Seibert, P., Stebel, K., and Stohl, A.: Estimation of the vertical profile of sulfur dioxide injection into the atmosphere by a volcanic eruption using satellite column measurements and inverse transport modeling, *Atmos. Chem. Phys.*, 8, 3881–3897, doi:10.5194/acp-8-3881-2008, 2008. 6565

Edmonds, M.: New geochemical insights into volcanic degassing, *Philos. T. R. Soc. A*, 366, 4559–4579, doi:10.1098/rsta.2008.0185, 2008. 6569, 6571

Galle, B., Johansson, M., Rivera, C., Zhang, Y., Kihlman, M., Kern, C., Lehmann, T., Platt, U., Arellano, S., and Hidalgo, S.: Network for Observation of Volcanic and Atmospheric Change (NOVAC), a global network for volcanic gas monitoring: network layout and instrument description, *J. Geophys. Res.-Atmos.*, 115, D05304, doi:10.1029/2009JD011823, 2010. 6557

Gonnermann, H. M. and Manga, M.: The fluid mechanics inside a volcano, *Ann. Rev. Fluid Mech.*, 39, 321–356, doi:10.1146/annurev.fluid.39.050905.110207, 2007. 6571

Graf, H.-F., Feichter, J., and Langmann, B.: Volcanic sulfur emissions: estimates of source strength and its contribution to the global sulfate distribution, *J. Geophys. Res.*, 102, 10727–10738, 1997. 6564

Gudmundsson, M., Thordarson, T., Höskuldsson, Á., Larsen, G., Björnsson, H., Prata, F., Oddsson, B., Magnússon, E., Högnadóttir, T., Petersen, G., Hayward, C., Stevenson, A., and Jónsdóttir, I.: Ash generation and distribution from the April–May 2010 eruption of Eyjafjallajökull, Iceland, *Scientific Reports*, 2, 2012. 6557, 6566, 6569

Harris, A. J. L., Gurioli, L., Hughes, E. E., and Lagreulet, S.: Impact of the Eyjafjallajökull ash cloud: a newspaper perspective, *J. Geophys. Res.*, 117, B00C08, doi:10.1029/2011JB008735, 2012. 6557

Highwood, E.-J. and Stevenson, D. S.: Atmospheric impact of the 1783–1784 Laki Eruption: Part II Climatic effect of sulphate aerosol, *Atmos. Chem. Phys.*, 3, 1177–1189, doi:10.5194/acp-3-1177-2003, 2003. 6556

Jonsson, S.: Fault slip distribution of the 1999 Mw 7.1 Hector Mine, California, earthquake, estimated from satellite radar and GPS measurements, *B. Seismolog. Soc. Am.*, 92, 1377–1389, doi:10.1785/0120000922, 2002. 6561

Inverting for volcanic SO₂ flux at high temporal resolution

M. Boichu et al.

Title Page

Abstract

Introduction

Conclusions

References

Tables

Figures

◀

▶

◀

▶

Back

Close

Full Screen / Esc

Printer-friendly Version

Interactive Discussion



- Kristiansen, N., Stohl, A., Prata, A., Richter, A., Eckhardt, S., Seibert, P., Hoffmann, A., Ritter, C., Bitar, L., Duck, T., and Stebel, K.: Remote sensing and inverse transport modeling of the Kasatochi eruption sulfur dioxide cloud, *J. Geophys. Res.*, 115, D00L16, doi:10.1029/2009JD013286, 2010. 6565
- 5 Krotkov, N. A., Schoeberl, M. R., Morris, G. A., Carn, S., and Yang, K.: Dispersion and lifetime of the SO₂ cloud from the August 2008 Kasatochi eruption, *J. Geophys. Res.-Atmos.*, 115, D00L20, doi:10.1029/2010JD013984, 2010. 6565
- Laursen, L.: Iceland eruptions fuel interest in volcanic gas monitoring, *Science*, 328, 410–411, doi:10.1126/science.328.5977.410, 2010. 6558, 6569
- 10 Lawson, C. L. and Hanson, R. J.: *Solving Least Squares Problems*, Society for Industrial and Applied Mathematics, Philadelphia, 1974. 6561
- Mastin, L. G., Guffanti, M., Servranckx, R., Webley, P., Barsotti, S., Dean, K., Durant, A., Ewert, J. W., Neri, A., Rose, W. I., Schneider, D., Siebert, L., Stunder, B., Swanson, G., Tupper, A., Volentik, A., and Waythomas, C. F.: A multidisciplinary effort to assign realistic source parameters to models of volcanic ash-cloud transport and dispersion during eruptions, *J. Volcanol. Geoth. Res.*, 186, 10–21, doi:10.1016/j.jvolgeores.2009.01.008, 2009. 6557
- 15 Mather, T.: Volcanoes and the atmosphere: the potential role of the atmosphere in unlocking the reactivity of volcanic emissions, *Phil. Trans. R. Soc. A*, 366, 4581–4595, 2008. 6556
- McCormick, M. P., Thomason, L. W., and Trepte, C. R.: Atmospheric effects of the Mt Pinatubo eruption, *Nature*, 373, 399–404, doi:10.1038/373399a0, 1995. 6556
- 20 Merucci, L., Burton, M., Corradini, S., and Salerno, G. G.: Reconstruction of SO₂ flux emission chronology from space-based measurements, *J. Volcanol. Geoth. Res.*, 206, 80–87, doi:10.1016/j.jvolgeores.2011.07.002, 2011. 6557
- Oddsson, B., Gudmundsson, M. T., Larsen, G., and Karlsdottir, S.: Monitoring of the plume from the basaltic phreatomagmatic 2004 Grimsvotn eruption: application of weather radar and comparison with plume models, *B. Volcanol.*, 74, 1395–1407, doi:10.1007/s00445-012-0598-9, 2012. 6565
- 25 Oppenheimer, C.: Ultraviolet sensing of volcanic sulfur emissions, *Elements*, 6, 87–92, doi:10.2113/gselements.6.2.87, 2010. 6557
- 30 Oppenheimer, C., Francis, P., and Stix, J.: Depletion rates of sulfur dioxide in tropospheric volcanic plumes, *Geophys. Res. Lett.*, 25, 2671–2674, 1998. 6559
- Oppenheimer, C., Pyle, D., and Barclay, J. E.: Volcanic degassing, *Special Publication*, Geological Society of London, 213, 2003. 6569

Inverting for volcanic SO₂ flux at high temporal resolution

M. Boichu et al.

Title Page

Abstract

Introduction

Conclusions

References

Tables

Figures

◀

▶

◀

▶

Back

Close

Full Screen / Esc

Printer-friendly Version

Interactive Discussion



- Oppenheimer, C., Scaillet, B., and Martin, R. S.: Sulfur degassing from volcanoes: source conditions, surveillance, plume chemistry and Earth system impacts, *Rev. Mineral. Geochem.*, 73, 363–421, doi:10.2138/rmg.2011.73.13, 2011. 6556
- Petersen, G. N., Bjornsson, H., and Arason, P.: The impact of the atmosphere on the Eyjafjallajökull 2010 eruption plume, *J. Geophys. Res.-Atmos.*, 117, D00U07, doi:10.1029/2011JD016762, 2012. 6557, 6559, 6560, 6566, 6570
- Robock, A.: Volcanic eruptions and climate, *Rev. Geophys.*, 38, 191–220, doi:10.1029/1998RG000054, 2000. 6556
- Robock, A. and Oppenheimer, C. E.: Volcanism and the Earth's atmosphere, *American Geophysical Union*, 139, 360 pp., 2003. 6556
- Rouil, L., Honoré, C., Vautard, R., Beekmann, M., Bessagnet, B., Malherbe, L., Meleux, F., Dufour, A., Elichegaray, C., Flaud, J.-M., Menut, L., Martin, D., Peuch, A., Peuch, V.-H., and Poisson, N.: Prev'air: an operational forecasting and mapping system for air quality in Europe, *B. Am. Meteorol. Soc.*, 90, 73–83, doi:10.1175/2008BAMS2390.1, 2009. 6558
- Schmidt, A., Carslaw, K. S., Mann, G. W., Rap, A., Pringle, K. J., Spracklen, D. V., Wilson, M., and Forster, P. M.: Importance of tropospheric volcanic aerosol for indirect radiative forcing of climate, *Atmos. Chem. Phys.*, 12, 7321–7339, doi:10.5194/acp-12-7321-2012, 2012. 6556
- Solomon, S., Portmann, R. W., Garcia, R. R., Randel, W., Wu, F., Nagatani, R., Gleason, J., Thomason, L., Poole, L. R., and McCormick, M. P.: Ozone depletion at mid-latitudes: coupling of volcanic aerosols and temperature variability to anthropogenic chlorine, *Geophys. Res. Lett.*, 25, 1871–1874, doi:10.1029/98GL01293, 1998. 6556
- Sparks, R. S. J., Bursik, M. I., Carey, S. N., Gilbert, J. S., Glaze, L. S., Sigurdsson, H., and Woods, A. W.: *Volcanic Plumes*, John Wiley & Sons, Chichester, 1997. 6565
- Stohl, A., Prata, A. J., Eckhardt, S., Clarisse, L., Durant, A., Henne, S., Kristiansen, N. I., Minikin, A., Schumann, U., Seibert, P., Stebel, K., Thomas, H. E., Thorsteinsson, T., Tørseth, K., and Weinzierl, B.: Determination of time – and height-resolved volcanic ash emissions and their use for quantitative ash dispersion modeling: the 2010 Eyjafjallajökull eruption, *Atmos. Chem. Phys.*, 11, 4333–4351, doi:10.5194/acp-11-4333-2011, 2011. 6558, 6569, 6570, 6573, 6585
- Surono, M., Jousset, P., Pallister, J., Boichu, M., Buongiorno, M. F., Budisantoso, A., Costa, F., Andreastuti, S., Prata, F., Schneider, D., Clarisse, L., Humaida, H., Sumarti, S., Bignami, C., Griswold, J., Carn, S., Oppenheimer, C., and Lavigne, F.: The 2010 explosive eruption of

Inverting for volcanic SO₂ flux at high temporal resolution

M. Boichu et al.

Title Page

Abstract

Introduction

Conclusions

References

Tables

Figures

◀

▶

◀

▶

Back

Close

Full Screen / Esc

Printer-friendly Version

Interactive Discussion



Java's Merapi volcano – a “100-year” event, *J. Volcanol. Geoth. Res.*, 241–242, 121–135, doi:10.1016/j.jvolgeores.2012.06.018, 2012. 6557

Tabazadeh, A., Drdla, K., Schoeberl, M. R., Hamill, P., and Toon, O. B.: From the Cover: Arctic “ozone hole” in a cold volcanic stratosphere, *Proc. Natl. Acad. Sci.*, 99, 2609–2612, doi:10.1073/pnas.052518199, 2002. 6556

Tarantola, A.: *Inverse Problem Theory and Methods for Model Parameter Estimation*, Society for Industrial and Applied Mathematics, Philadelphia, 2005. 6561

Theys, N., Champion, R., Clarisse, L., Brenot, H., van Gent, J., Dils, B., Corradini, S., Merucci, L., Coheur, P.-F., Van Roozendael, M., Hurtmans, D., Clerbaux, C., Tait, S., and Ferrucci, F.: Volcanic SO₂ fluxes derived from satellite data: a survey using OMI, GOME-2, IASI and MODIS, *Atmos. Chem. Phys. Discuss.*, 12, 31349–31412, doi:10.5194/acpd-12-31349-2012, 2012. 6557

Thordarson, T. and Self, S.: Atmospheric and environmental effects of the 1783–1784 Laki eruption: a review and reassessment, *J. Geophys. Res.-Atmos.*, 108, 4011, doi:10.1029/2001JD002042, 2003. 6557

Veeffkind, J.-P., Aben, I., McMullan, K., Förster, H., de Vries, J., Otter, G., Claas, J., Eskes, H., de Haan, J., Kleipool, Q., van Weele, M., Hasekamp, O., Hoogeveen, R., Landgraf, J., Snel, R., Tol, P., Ingmann, P., Voors, R., Kruizinga, B., Vink, R., Visser, H., and Levelt, P. F.: TROPOMI on the ESA Sentinel-5 Precursor: a GMES mission for global observations of the atmospheric composition for climate, air quality and ozone layer applications, *Remote Sens. Environ.*, 120, 70–83, 2012. 6572

Vernier, J.-P., Thomason, L. W., Pommereau, J.-P., Bourassa, A., Pelon, J., Garnier, A., Hauchecorne, A., Blanot, L., Trepte, C., Degenstein, D., and Vargas, F.: Major influence of tropical volcanic eruptions on the stratospheric aerosol layer during the last decade, *Geophys. Res. Lett.*, 38, 12807, doi:10.1029/2011GL047563, 2011. 6556

Webley, P. and Mastin, L.: Improved prediction and tracking of volcanic ash clouds, *J. Volcanol. Geoth. Res.*, 186, 1–9, doi:10.1016/j.jvolgeores.2008.10.022, 2009. 6556

Inverting for volcanic SO₂ flux at high temporal resolution

M. Boichu et al.

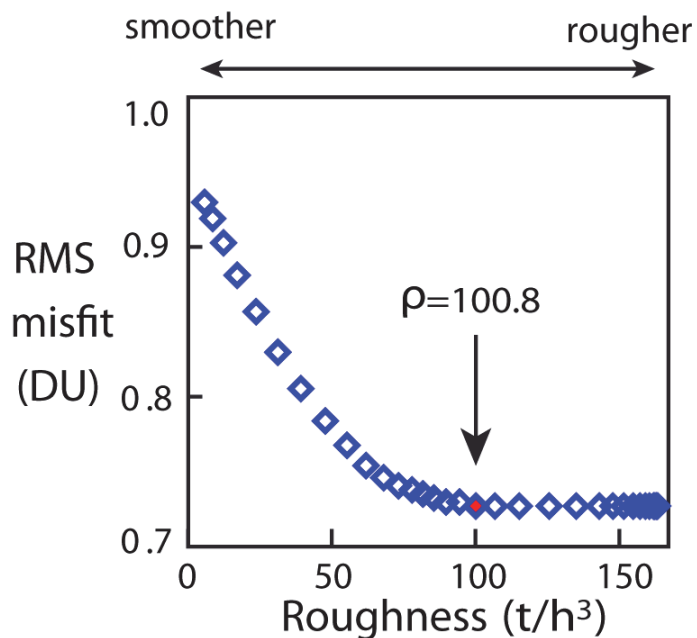


Fig. 1. Normalised RMS misfit (in Dobson Units) as a function of solution roughness (t/h^{-3}), using the complete time-series of IASI satellite observations (from 4 to 12 May 2010) in the inversion procedure. The optimal roughness is indicated in red.

Title Page

Abstract

Introduction

Conclusions

References

Tables

Figures

◀

▶

◀

▶

Back

Close

Full Screen / Esc

Printer-friendly Version

Interactive Discussion



Inverting for volcanic SO₂ flux at high temporal resolution

M. Boichu et al.

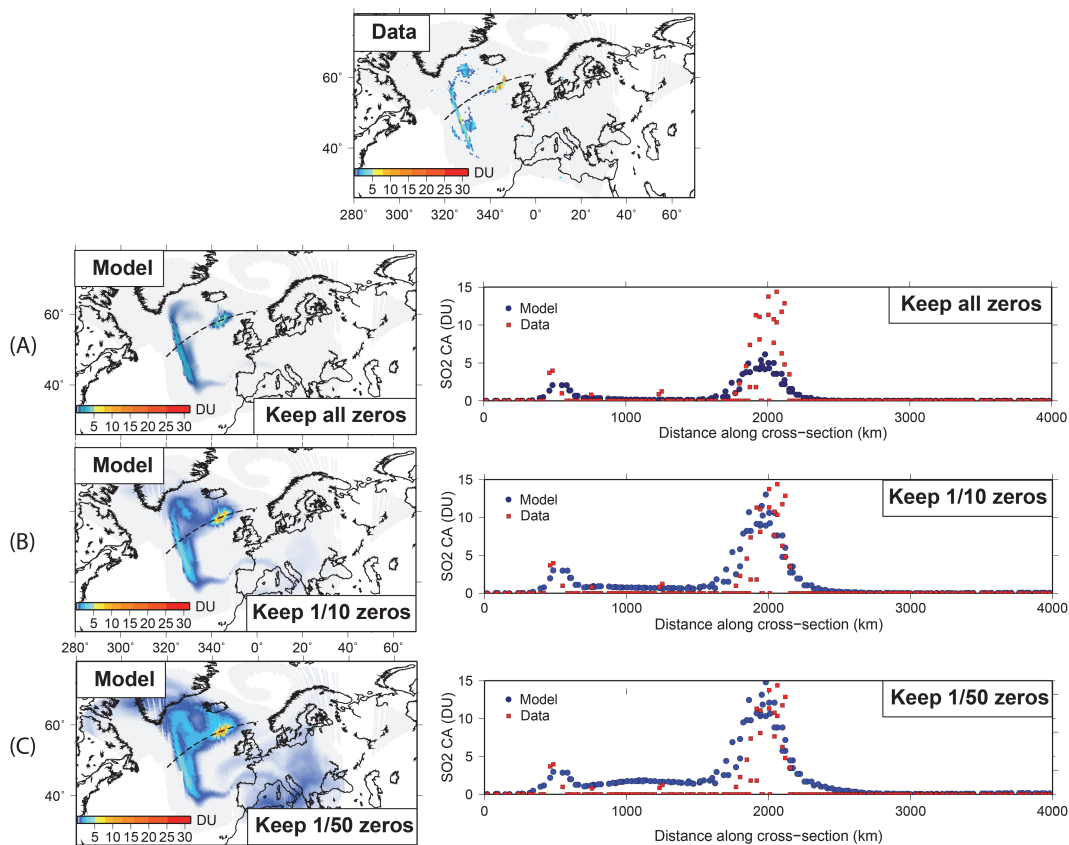


Fig. 2. Comparison of observed (top) and modeled (bottom) plume SO₂ column amount (DU) maps for various amounts of random data decimation before the inversion procedure: **(A)** all null observations yielding a zero SO₂ column amount are kept in the inversion scheme, **(B)** one out of ten null observations are kept, **(Bottom)** one out of fifty null observations are kept. **(C)** Values of (red) observed and (blue) modeled SO₂ column amounts (DU) along the plume cross-section (dashed line on maps) retrieved according to data sampling. Maps are associated with IASI observations acquired on 9 May 2010 over a 12 h window centered at 00:00 UTC.

Title Page

Abstract

Introduction

Conclusions

References

Tables

Figures

◀

▶

◀

▶

Back

Close

Full Screen / Esc

Printer-friendly Version

Interactive Discussion



Inverting for volcanic SO_2 flux at high temporal resolution

M. Boichu et al.

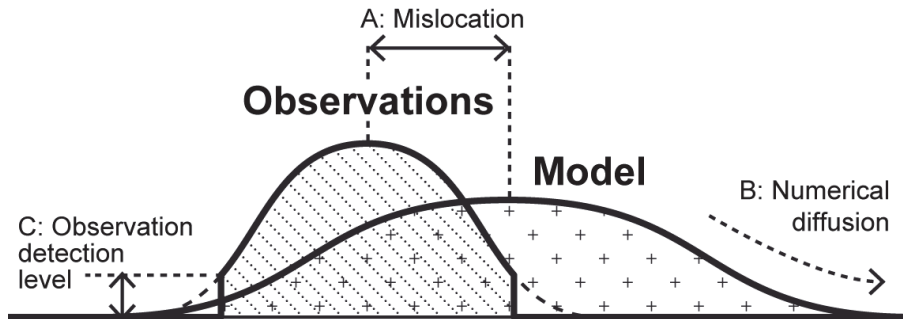


Fig. 3. Schematic cross-section of observed and modeled volcanic plume.

Title Page

Abstract

Introduction

Conclusions

References

Tables

Figures

◀

▶

◀

▶

Back

Close

Full Screen / Esc

Printer-friendly Version

Interactive Discussion



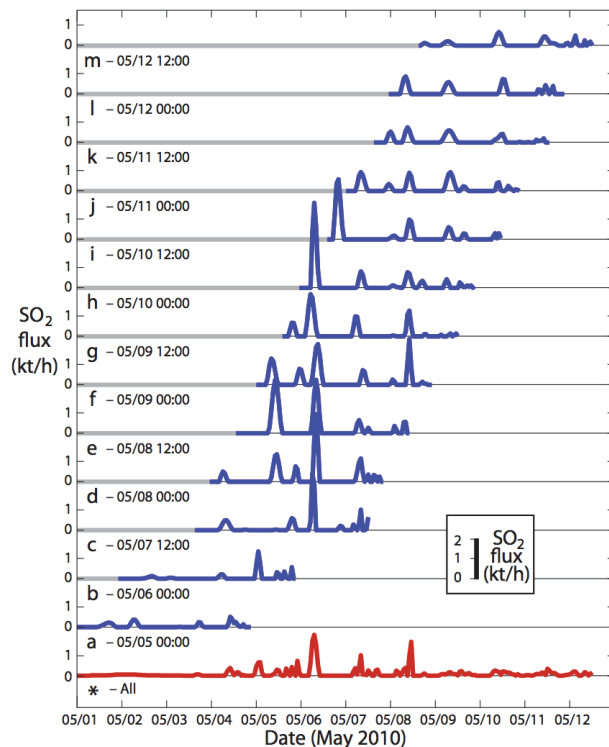


Fig. 4. Time-series of the SO_2 flux released during the Eyjafjallajökull eruption (May 2010) reconstructed using (a to m) single- or (*) multiple-image inversion. Each time-series (from a to m) corresponds to a SO_2 column amount map gathering IASI measurements acquired over a twelve hour time-window, centered on the date indicated on the left. The multiple-image inversion scheme integrates all thirteen IASI maps. SO_2 emissions released more than 3.5 days prior to the first acquisition time of the considered IASI image (grey lines) are not constrained by the inversion procedure.

Inverting for volcanic SO_2 flux at high temporal resolution

M. Boichu et al.

Title Page

Abstract Introduction

Conclusions References

Tables Figures

◀ ▶

◀ ▶

Back Close

Full Screen / Esc

Printer-friendly Version

Interactive Discussion



Inverting for volcanic SO₂ flux at high temporal resolution

M. Boichu et al.

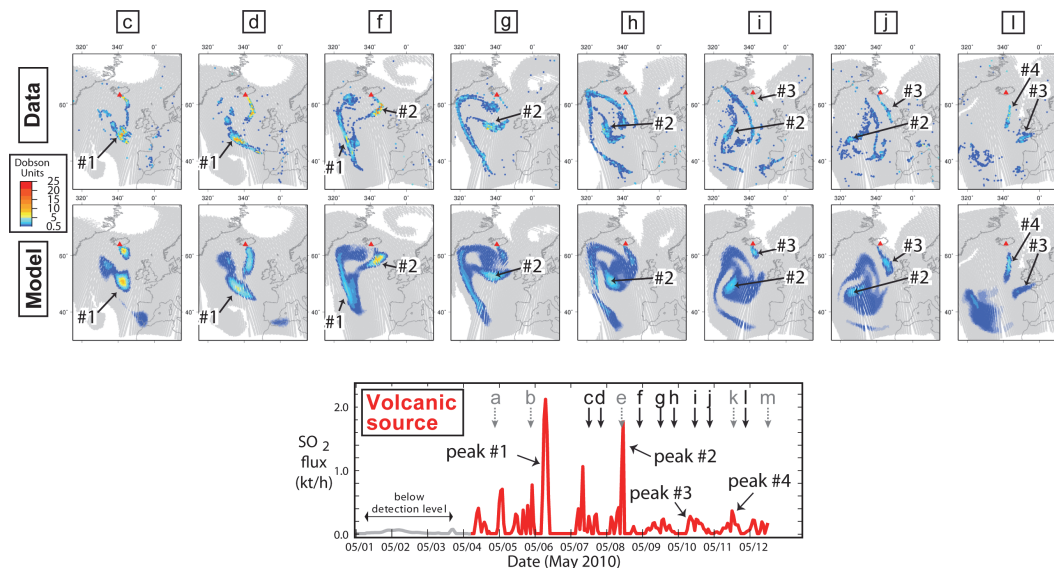


Fig. 5. Comparison of observed and modeled atmospheric evolution of the Eyjafjallajökull plume in May 2010. Data: maps of SO₂ column amounts (CA in DU) derived from the processing of IASI satellite observations. Model: maps of SO₂ CA simulated with CHIMERE chemistry-transport model, using the source reconstructed by multiple-image inversion (bottom plot). Regions in grey indicate column amounts less than 0.5 DU, which corresponds to the detection threshold in IASI processing (see Sect. 2.2 for details). Source: time-series of the SO₂ flux (kt h⁻¹) retrieved from the inversion procedure using the thirteen IASI images available for the period from 1 to 12 May 2010 (numbered **a** to **m** and indicated with arrows). The complete time-series of observed and modeled maps is available in Appendix (Figs. A1 and A2). As illustrated by a few examples, peaks in the SO₂ flux create dense puffs in the plume which can be tracked up to 6 days after their emission.

[Title Page](#)
[Abstract](#)
[Introduction](#)
[Conclusions](#)
[References](#)
[Tables](#)
[Figures](#)
[Back](#)
[Close](#)
[Full Screen / Esc](#)
[Printer-friendly Version](#)
[Interactive Discussion](#)

Inverting for volcanic SO₂ flux at high temporal resolution

M. Boichu et al.

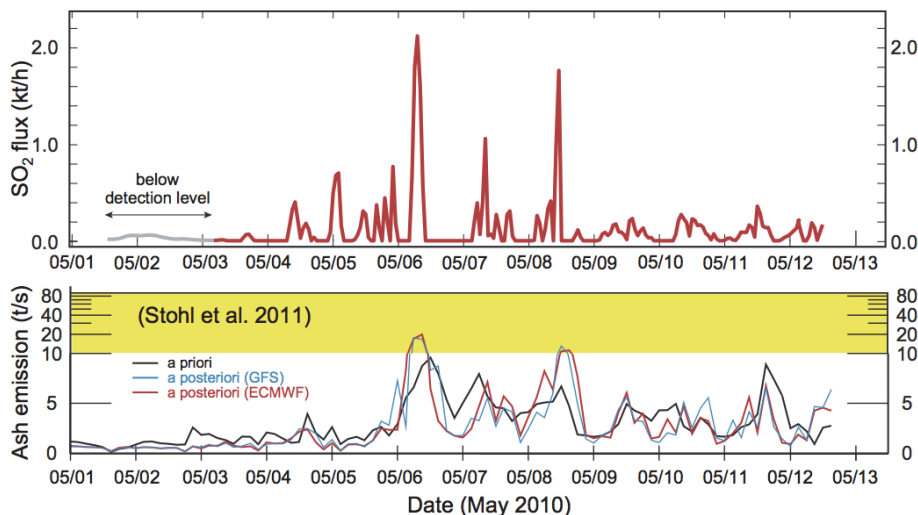


Fig. 6. Comparison between SO₂ and ash emissions during the Eyjafjallajökull eruption of May 2010. (Top) Time-series of the SO₂ flux (kt h⁻¹) (this study). (Bottom) Ash emission rate (t s⁻¹) from the inverse modeling of Stohl et al. (2011) (The black line represents the a-priori, blue and red lines the a-posteriori using respectively the GFS and ECMWF meteorological models. Note the mix of linear and logarithmic scales in the ordinate axis.)

Title Page

Abstract

Introduction

Conclusions

References

Tables

Figures

◀

▶

◀

▶

Back

Close

Full Screen / Esc

Printer-friendly Version

Interactive Discussion



Inverting for volcanic SO₂ flux at high temporal resolution

M. Boichu et al.

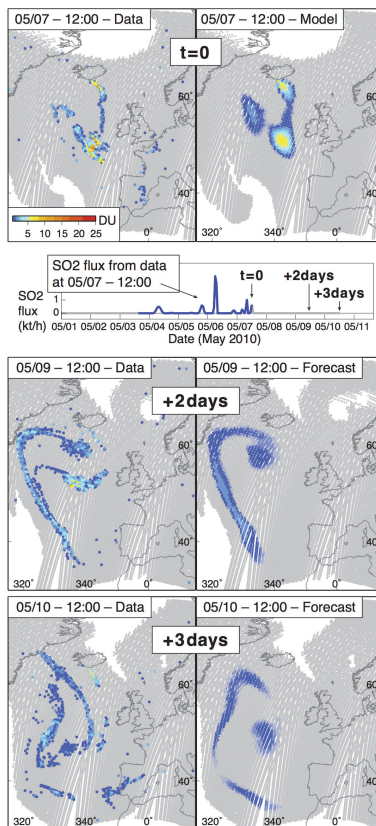


Fig. 7. Forecast at (middle) +2 days and (bottom) +3 days of the SO₂ plume using the source reconstructed from (top) the IASI image acquired on 7 May 2010 on a 12 h time-window centered at 12:00 UTC (source **c** in Fig. 4).

Title Page

Abstract

Introduction

Conclusions

References

Tables

Figures

⏪

⏩

◀

▶

Back

Close

Full Screen / Esc

Printer-friendly Version

Interactive Discussion



Inverting for volcanic SO₂ flux at high temporal resolution

M. Boichu et al.

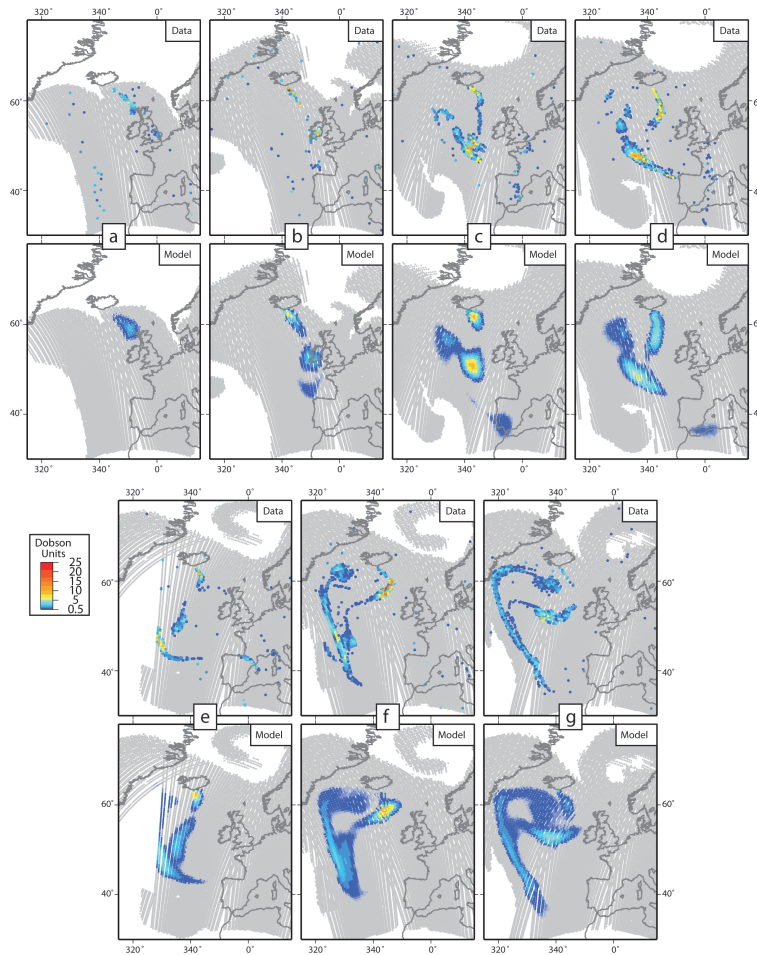


Fig. A1. Complete time-series of observed and modeled maps, numbered **a** to **m** in Fig. 5, which illustrates the atmospheric evolution of the Eyjafjallajökull plume from 1 to 12 May 2010. The reader is referred to the legend of Fig. 5 for details.

Inverting for volcanic SO₂ flux at high temporal resolution

M. Boichu et al.

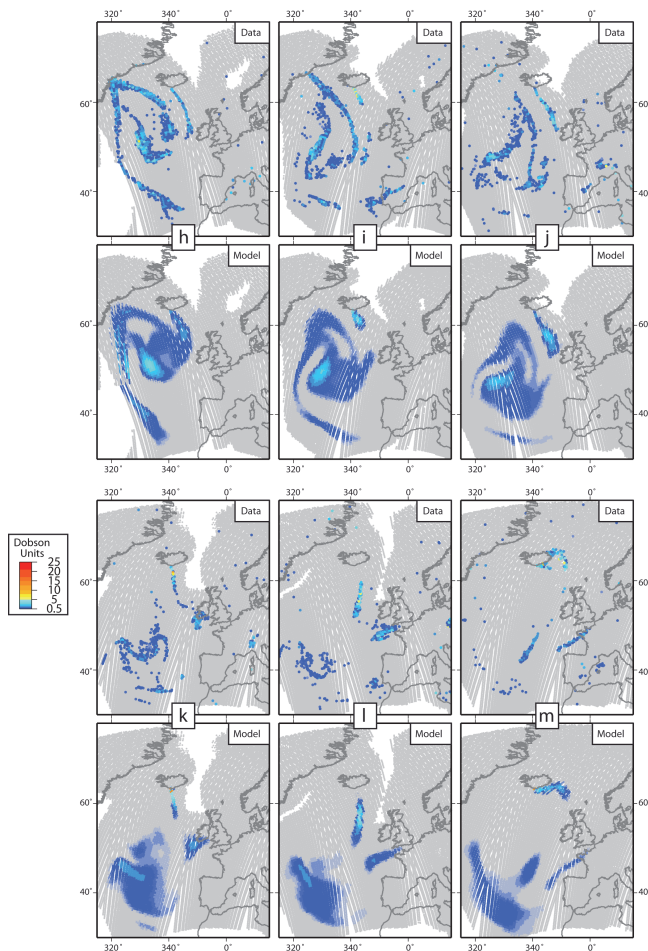


Fig. A2. Continuation of Fig. A1 including maps numbered h to m.

Title Page

Abstract

Introduction

Conclusions

References

Tables

Figures

◀

▶

◀

▶

Back

Close

Full Screen / Esc

Printer-friendly Version

Interactive Discussion

